BLD10/CEP135 is a microtubule-associated protein that controls the formation of the flagellum central microtubule pair

Zita Carvalho-Santos[1*],Pedro Machado[1*], Inês Alvarez-Martins[1], Susana M Gouveia[1], Swadhin C Jana[1], Paulo Duarte[1], Tiago Amado[1], Pedro Branco[1], Micael C. Freitas[2], Sara T.N. Silva[2, 3], Claude Antony [4], Tiago M. Bandeiras[2, 3], Mónica Bettencourt-Dias[1]

[1] Instituto Gulbenkian de Ciência, Rua da Quinta Grande 6, 2780-156 Oeiras, Portugal
[2] IBET, Apartado 12, 2781-901 Oeiras, Portugal
[3] Instituto de Tecnologia Química e Biológica, Universidade Nova de Lisboa, Av. da República, 2780-157 Oeiras, Portugal
[4] European Molecular Biology Laboratory, Heidelberg, Germany
* These authors contributed equally

Authors for correspondence:
Mónica Bettencourt-Dias, Instituto Gulbenkian de Ciência, Rua Oeiras, Portugal
E-mail: mdias@igc.gulbenkian.pt
Zita Carvalho-Santos, Instituto Gulbenkian de Ciência, Rua Oeiras, Portugal
Email: zitasantos@igc.gulbenkian.pt

Summary

Cilia and flagella are structures involved in a variety of developmental processes and human diseases, including ciliopathies and sterility. Here we investigate how the central microtubule (MT) pair, that controls flagellum motility, is formed. We show that this structure assembles inside a small cilium surprisingly early during *Drosophila* spermatogenesis, prior to the meiotic divisions. First, a singlet MT forms within the basal body/ciliary complex. This structure is maintained within the centrosome through meiosis, until the stage of flagellum assembly, where the second MT of the pair nucleates close to it. We and others have shown that, in *Drosophila,* loss of BLD10/CEP135, a conserved player of centriole biogenesis, leads to shorter centrioles and loss of the central MT pair. We now show that *Drosophila* Bld10 directly binds and stabilises MTs through its N-terminal domain. Moreover, in *Bld10* mutants the singlet MT is not formed; consequently, the central pair is not assembled, leading to male sterility. This work describes a genetically tractable system to study motile cilia biogenesis and provides an explanation for BLD10/CEP135´s role in the assembly of highly stable MT-based structures, such as centrioles and motile axonemes.

Introduction

Cilia are microtubule (MT)-based organelles involved in a variety of processes, such as cell motility, fluid flow, and sensing mechanical stimuli and signalling molecules. Defects in cilia can cause multiple human diseases, including obesity, retinal degeneration, *situs inversus,* and male infertility (Bettencourt-Dias et al., 2011; Nigg and Raff, 2009). At the base of each cilium there is at least one modified centriole, the basal body (BB), which templates the growth of the axoneme, the MT-based axoneme of cilia. Centrioles are also essential for the formation of centrosomes, the primary MT organiser of the cell (Bettencourt-Dias et al., 2011; Nigg and Raff, 2009). Yet, little is still known about the molecular mechanisms that govern the switch of centrioles to basal bodies, organelles required to form cilia.

Cilia can exist as motile or immotile structures. Most motile cilia, such as those of green algae, protozoa, sperm, and respiratory tract cells, have a pair of central MTs within the lumen of their axoneme to coordinate cilia motility (Fliegauf et al., 2007). In fully assembled axonemes, this central MT pair starts at the most proximal part of the axoneme, a region called the transition zone. Both green algae and ciliates contain well-defined structures such as stellate fibres and transitional plates in the transition zone of their motile cilia/flagella (Dute and Kung, 1978; Geimer and Melkonian, 2004; Hibberd, 1975). However, the universality and function of those structures in central pair assembly is unknown. Microtubule regulators are likely to control the assembly of the central MT pair; indeed γ-tubulin is required for this process in protozoa (McKean et al., 2003; Silflow et al., 1999). Although studies in sea urchin suggested heterotrimeric kinesin-2 to have a role in central MT pair assembly through intraflagellar transport (Morris and Scholey, 1997), little is still known about the structural and molecular mechanisms that underlie this process.

Drosophila melanogaster mutants for Bld10, a conserved player in centriole biogenesis, have short centrioles and the majority of sperm flagella lack the central MT pair (Carvalho-Santos et al., 2010; Mottier-Pavie and Megraw, 2009). In *Chlamydomonas* and *Paramecium*,

BLD10/CEP135 localizes close to the centriolar MTs at the spoke tips of the cartwheel, a nine-fold symmetric structure present at the base of centrioles that enforces their symmetry (Hiraki et al., 2007; Jerka-Dziadosz et al., 2010; Matsuura et al., 2004). Depletion of BLD10/CEP135 in those organisms severely impairs basal body assembly (Hiraki et al., 2007; Jerka-Dziadosz et al., 2010; Matsuura et al., 2004). In human culture cells, CEP135 is required for centriole assembly and localizes to the cartwheel, the centriolar walls, and the lumen of the centriole distal region (Kleylein-Sohn et al., 2007). Altogether, this data strongly indicates that BLD10/CEP135 has a MT-related function that underlies its role in centriole assembly. Moreover, its localization at the most distal part of the centrioles in both human and *Drosophila* suggests a role in the initiation of central MT pair assembly (Carvalho-Santos et al., 2010; Kleylein-Sohn et al., 2007; Mottier-Pavie and Megraw, 2009).

To understand how the central MT pair is assembled, we first characterized this process in detail in *Drosophila* spermatogenesis. We show that this structure starts to assemble prior to the meiotic divisions, with nucleation of a singlet microtubule within the basal body of a small cilium. The second MT of the pair assembles much later, at the spermatid stage. To investigate the molecular mechanisms controlling the assembly of this structure we explored the function of BLD10/CEP135. We demonstrate that Bld10 is required for the first steps of central MT pair formation through the assembly of the singlet MT. Moreover, we show that this role depends on Bld10´s ability to bind and stabilize MTs. Our work describes a genetically tractable system to study motile cilia assembly and provides a molecular mechanism that explains BLD10/CEP135 role in the assembly of highly stable MT-based structures, such as centrioles and motile axonemes.

Results

A singlet MT precedes the formation of the central MT pair

To elucidate the process of central MT pair assembly in animal motile cilia, we used the fruit fly, a model organism that assembles these structures exclusively in sperm cells. We began by performing a morphologically detailed characterization of *Drosophila* spermatogenesis using serial sectioning, transmission electron microscopy (TEM) and electron tomography. It is known that *Drosophila* sperm formation starts when a stem cell divides asymmetrically to originate a gonial cell (**Figure 1 A**) (Fuller, 1998; Tates, 1971). Each gonial cell undergoes four consecutive rounds of mitotic divisions resulting in a cyst of 16 interconnected primary spermatocytes (**Figure 1 A**). These will then undergo a long G2 phase, during which centrioles elongate to more than 6 times the size of their somatic counterparts (**Figure 1 A**) (Fuller, 1998; Tates, 1971). During this stage all four centrioles migrate to the cell membrane to become basal bodies and assemble a small cilium (**Figure 1 B'**) (Fritz-Niggli and Suda, 1972; Fuller, 1998; Tates, 1971). As this is the first stage of spermatogenesis where an axoneme forms, we characterized the BB and cilium structures in detail using tomography and serial sectioning (**Figure 1 B-C, S1** and **Movies S1-2**). We observed one MT within the BB lumen that, in some cases, extended uninterruptedly into the cilium, which we refer to as singlet MT throughout the text (**Figures 1 B-C, S1,** and **Movies S1-2**). This MT, which we refer to as singlet MT throughout the text, likely corresponds to a tube previously observed by Tates (1971) in single sections of the basal body distal region, whose nature and length was unknown at the time. We observed variability regarding the presence and length of the singlet MT, with cases where the singlet MT is observed just within the basal body and others where it spans into the cilium (**Figures 1 B-C, 3 A-B, S1,** and **Movies S1-2**). It is thus conceivable that the singlet MT forms during the process of cilium assembly first within the BB and then elongates into the axoneme (**Figure S7**).

Since cilia of primary spermatocytes are immotile (they lack dynein arms), and immotile cilia are usually devoid of central MTs, the presence of a singlet MT in the basal body/ciliary lumen was unexpected. We hypothesized that the singlet could be a precursor of the central

MT pair of sperm flagella. To test this we followed the fate of the singlet MT in the subsequent developmental stages. Just before meiosis, we observed the internalization of the whole complex consisting of basal body, axoneme and ciliary membrane (**Figure 1 B'** and **D**) and migration to the poles of the spindle, where it participated in cell division as a centrosome (**Figure 1 E**). We observed that, not only the cilium, but also the singlet MT was retained during meiotic divisions (**Figure 1 E''**), similarly to what was previously described (Fritz-Niggli and Suda, 1972; Tates, 1971).

We then investigated the presence of the singlet MT in the basal bodies of the early spermatid flagellum. At this stage the axoneme of the flagellum is known to contain a central MT pair. We observed that the lumen of these basal bodies also contained a singlet MT that extended into the axoneme, where a second microtubule was formed. Together they gave rise to the well known central MT pair (**Figures 2, S2** and **Movies S3-S4**). This data strongly supports the hypothesis that the tubule observed within the basal bodies of the cilium and flagellum is a microtubule. These results suggest that, during *Drosophila* spermatogenesis, central MT pair assembly starts within the basal body of primary spermatocytes, i.e., well before what was previously suspected, and that the singlet MT is the precursor for central MT pair formation in the sperm flagellum.

Bld10 is required for initiation of central pair assembly

To our knowledge, no molecules have been described to be involved in the initiation of central MT pair assembly in animals. Recent work showed that *Drosophila Bld10* mutants lack the central MT pair (Carvalho-Santos et al., 2010; Mottier-Pavie and Megraw, 2009). Moreover, Bld10 localizes both at the centriole and at the most distal region of the basal body during cilia formation and throughout spermatogenesis, suggesting a role in central MT pair assembly and/or maintenance (Blachon et al., 2009; Carvalho-Santos et al., 2011; Mottier-Pavie and Megraw, 2009). We reasoned that if Bld10 is involved in initiating the assembly of the central MT pair, it should be required for the assembly of the singlet MT. To test this

hypothesis we investigated the basal body/ciliary structure of wild type (WT) vs. Bld10 mutant (*Bld10*) from G2 spermatocytes and spermatids. In WT G2 spermatocytes, 48% of basal body/ciliary complexes contained a singlet MT (**Figure 3 A**-**B**). We figured that if this structure is a precursor of the central MT pair, most basal bodies in early spermatids, should contain a singlet MT. Indeed, 80% of the WT basal bodies in early spermatids did contain this structure (**Figure 3 C**-**D**). The absence of the singlet MT in the remainder 20% may either reflect experimental constrains related to structural instability, or most likely, be associated with analysis of sections where the singlet MT is not present, such as those at proximal BB regions (**Figures 2** and **S2**). In contrast to what we observed for the WT, in *Bld10* only 14% of basal body/ciliary structures of G2 spermatocytes had the singlet MT (**Figure 3 A**-**B**) and the majority of basal bodies in early spermatids (**Figure 3 C**-**D**) did not contain it. Bld10 is thus required for the assembly/stabilization of the singlet MT throughout spermatogenesis. Moreover, since the majority of *Bld10* flagellum axonemes lack the central MT pair (Carvalho-Santos et al., 2010; Mottier-Pavie and Megraw, 2009) these results support the hypothesis of the singlet MT being a precursor for central MT pair formation.

Bld10 directly binds and stabilizes MTs

BLD10/CEP135 was shown to localize to the cartwheel spokes and to be a critical player in centriole assembly at the level of centriole elongation and cartwheel biogenesis on a variety of species (Carvalho-Santos et al., 2010; Hiraki et al., 2007; Jerka-Dziadosz et al., 2010; Kleylein-Sohn et al., 2007; Matsuura et al., 2004; Mottier-Pavie and Megraw, 2009). It is possible that one function of Bld10 at the cartwheel spokes is to stabilize centriole MTs. This evidence together with the data we presented in the previous section suggests a role for Bld10 in MT regulation. To test this hypothesis we first investigated if BLD10/CEP135 is a MT-associated protein. Immuno-EM data on *Chlamydomonas* showed that the N-terminus of the protein localizes close to the centriolar MT triplets, at the most distal part of the cartwheel spokes (Hiraki et al., 2007). A similar result was described in *Paramecium*, where GFP-PtBLD10

was detected in close proximity to the MT triplets using an anti-GFP antibody (Jerka-Dziadosz et al., 2010). Moreover, the fact that BLD10/CEP135 N-terminus is conserved suggests this region to be functionally important, for instance, in MT binding (Carvalho-Santos et al., 2010).

We performed a MT pelleting assay to evaluate the MT binding capacity of the Bld10 N-terminal region *in vitro* (**Figure 4**). We expressed and purified a Bld10 fragment from *E. coli* encompassing the N-terminal Conserved Region 1 (His-N-Bld10, residues 1-163). Upon incubation of this Bld10 fragment with taxol-stabilized MTs, we observed that all His-N-Bld10 protein co-sedimented with the polymerized MT fraction (pellet (**P**) in **Figure 4 B**). In contrast, His-Ethe-1, a mitochondrial protein lacking known MT binding domains, was mostly found in the supernatant, which contains non-polymerized tubulin (supernatant (**S**) in **Figure 4 B**) (Braun et al., 2009). We observed consistent results in a MT overlay assay, by incubating a membrane containing the proteins of interest with stabilized MTs (**Figure 4 C**) (Inoue et al., 2000). In contrast to the negative controls His-Ethe-1 and BSA, His-N-Bld10 bound strongly to MTs similarly to the MT binding domain (MBD) of SAS4/CPAP (GST-MBD-CPAP), a conserved centriolar protein known to be required for centriole MT elongation that we used in this assay as positive control (**Figure 4 C**) (Hsu et al., 2008; Hung et al., 2004; Kohlmaier et al., 2009; Schmidt et al., 2009; Tang et al., 2009). These data strongly indicates that Bld10 is a MT-associated protein (MAP) that binds MTs directly, at least via its conserved N-terminal.

In order to further explore the above-described *in vitro* results, we evaluated whether this protein also binds MTs in *Drosophila* culture cells. In a WT background, *Drosophila* Bld10 has only been detected at centrioles (Blachon et al., 2009; Carvalho-Santos et al., 2010; Dobbelaere et al., 2008; Mottier-Pavie and Megraw, 2009). Previous studies showed that in human culture cells, SAS4/CPAP localizes to centrioles but it can also bind cytoplasmic MTs when overexpressed (Hsu et al., 2008). We thus addressed if this protein also had this ability by analyzing GFP-Bld10 localization upon expression in *Drosophila* culture cells. As previously described, GFP-Bld10 decorates the centrioles, shown by co-localization with the centrosomal

protein D-PLP, when expressed at low levels (Carvalho-Santos et al., 2010; Dobbelaere et al., 2008) (**Figure S3 A-B**). Interestingly, if expressed at higher levels GFP-Bld10 co-localizes with acetylated tubulin, indicating it can also bind MTs in cells (**Figures 5 B** and **S3 C)**. This binding is likely mediated by Bld10 N-terminal region, as this domain alone also binds cytoplasmic MTs when highly expressed in culture cells, but not the middle (GFP-M-Bld10), the conserved C-terminal (GFP-C-Bld10), or a truncated version lacking the N-terminus region (GFP-ΔN-Bld10) (**Figures 5 A-B** and **S3 C**). Additionally, all constructs also localized to the centrosome, suggesting the existence of different targeting regions (**Figure S3 B**). Altogether, our results suggest that Bld10 N-terminal region is important for its interaction with MTs, both *in vitro* and in cells.

In the course of our experiments we also observed that cells expressing GFP-Bld10 exhibited a 12-fold increase in MT bundle frequency when compared to control cells, suggesting a role for Bld10 in MT stabilization (**Figure 5 B-C**). We investigated if the MTs in these cells were more stable, i.e., resistant to colchicine-induced MT depolymerization. We found that GFP-Bld10 protein protected cytoplasmic MTs during the course of this treatment (**Figure 5 B-C**). In the presence of colchicine, 90% of control cells were either devoid of MTs or had very short ones, whereas only 10% of GFP-Bld10-expressing exhibited such phenotype (**Figure 5 B-C**). In these cells, both normal arrays as well as bundles of MTs were resistant to colchicine treatment (**Figure 5 B-C**). Bld10 stabilizing capacity is likely mediated by the N-terminal region as a similar phenotype was obtained upon expression of this domain alone, but not upon expression of the GFP-ΔN, M or C-Bld10 constructs (**Figure 5**). Lastly, TEM-based analysis revealed the presence of MT bundles surrounded by electron dense material in cells expressing either GFP-Bld10 or GFP-N-Bld10 (**Figure S4**). Together, these results suggest that, similarly to other MAPs, Bld10 binds to and stabilizes MTs in *Drosophila* cells.

Bld10 stabilizes the central MT pair *in vivo*

Drosophila Bld10 localizes at the centriole cartwheel, lumen and walls and also at the base of the axoneme, but not along the axoneme (Carvalho-Santos et al., 2010; Mottier-Pavie and Megraw, 2009). The results discussed in previous sections suggest that Bld10 acts in central MT pair assembly through its stabilization within the basal body and proximal part of the axoneme.

We next addressed whether Bld10 MT-stabilizing activity was relevant for its role *in vivo*. Since the N-terminus of this protein has strong MT-stabilizing activity, and an N-terminal truncation version of Bld10 loses this activity (**Figure 5**), we evaluated if this domain is important for central MT pair assembly in sperm flagella. We used the polyubiquitin promoter, a constitutive promoter routinely used in the fly to drive the expression of GFP-Bld10 or GFP-ΔN-Bld10 in *Bld10* mutants (Martinez-Campos et al., 2004; Rodrigues-Martins et al., 2007a; Rodrigues-Martins et al., 2007b). Both constructs were expressed at similar levels in testes of a *Bld10* mutant background (**Figure 6 A**) and localized to the centriole/basal body (**Figure S5**). To quantitatively access the functionality of these proteins in the assembly of the central MT pair, we scored defects in this structure in fully assembled flagella. GFP-Bld10 rescued the central MT pair phenotype to 60% of the WT (**Figure 6 C-D**). However, the GFP-ΔN-Bld10 could only rescue central MT pair formation by 37%. In agreement, this Bld10-truncated version was less efficient in rescuing male *Bld10* mutant fertility as compared to the full length molecule (**Figure 6 B**). Together, these results indicate that Bld10 N-terminus domain, which binds and stabilizes MTs, contributes to Bld10 activity in the formation of the sperm flagella central MT pair. Thus, Bld10 is likely to mechanistically act in central pair formation through MT stabilization.

To further test if Bld10 functions in central MT pair formation through a direct role on MTs, we addressed if the *Bld10* mutant phenotype was more pronounced by exposure to low doses of colchicine. Colchicine interferes with new MT-polymerization, hence its usefulness in tackling dynamic processes. Assuming the singlet MT formation as the first step in central MT

pair assembly, the whole process of assembling those MTs and motile flagella lasts approximately 6-7 days (Fuller, 1998). We fed newly eclosed males on a low dose of colchicine (1 μM) for 7-9 days, so that the early dynamic stages of central MT pair assembly would be exposed to this drug and we could look at its consequences quantitatively. At this concentration we did not observe any defects in central pair assembly or maintenance in WT flies (**Figure S6**). However, *Bld10* mutant flies showed a significant increase in the severity of their phenotype (**Figure S6**), strongly supporting our hypothesis that Bld10 functions in central MT pair assembly through MT stabilization. No defects were observed in other MT populations, such as the axonemal outer MT doublets, supporting a specific role for Bld10 in initiating central microtubule pair assembly..

Discussion

The central MT pair is an essential and highly specialized structure present in motile cilia required for coordinated motility. It is known that axonemal MT doublets extend from the basal body MT triplets. However, the biogenesis of the central MT pair is conceptually more complex and the morphological and molecular changes that occur during this process are yet to be characterized. Building on influential morphological work that described spermatogenesis in the fruit fly (Fritz-Niggli and Suda, 1972; Tates, 1971), we established *Drosophila* spermatogenesis as a genetically tractable system to study central MT pair formation. We show that the assembly of this structure initiates prior to the meiotic divisions, much earlier than previously assumed. During that stage, a singlet MT forms within the basal body of a small cilium in G2 spermatocytes (**Figure 1**, summarized in **Figure S7**). This MT is likely very stable as it is present throughout meiotic divisions and until axoneme extension (**Figures 1-2** and **S7**). In early spermatids, the stage at which flagellum assembly takes place, a second MT appears close to the singlet, and completes central MT pair formation (**Figures 2** and **S7**). Bld10 emerged as an ideal candidate to regulate central MT pair formation as Bld10

mutants lack this structure and the protein localizes to both the lumen and distal regions of the centriole/basal body (Carvalho-Santos et al., 2010; Mottier-Pavie and Megraw, 2009). Accordingly, we demonstrate that spermatogenesis in *Bld10* mutants is carried out without assembly of the singlet MT, thus impacting on central MT pair biogenesis (**Figure 3**). We show that Bld10 is a MAP whose overexpression leads to MT stabilization in culture cells (**Figures 4** and **5**). Finally, we directly link MT stabilizing activity of Bld10 to central MT pair assembly as: i) its N-terminus, which binds and stabilizes MTs, contributes to this process, and that ii) exposure to colchicine during central MT pair formation accentuates the *Bld10* mutant phenotype (**Figures 6** and **S6**).

Our morphological findings of central MT pair assembly during *Drosophila* spermatogenesis are summarized in **Figure S7**. The identification and analysis of different stages of this process, using tomography, TEM serial and single sections (**Figures 1-3, S1-2** and **Movies S1-4**), suggests this assembly is much more dynamic than we anticipated (**Figure S7**). We propose that central MT pair biogenesis starts with the formation/stabilization of a singlet MT precursor within the lumen of the basal body. The detailed analysis of this process raises several important questions, including where the first singlet MT is nucleated from, and whether it actively participates in the assembly of the second MT of the pair. The identification of singlet MT and/or central pair markers that do not localize to other centriole/axoneme structures will allow further mechanistic studies of central MT pair assembly in a less laborious fashion than as it is now with electron microscopy.

The observation that a singlet MT forms within the basal body as a precursor for the biogenesis of central MT pair of motile axoneme, implies a broader role of the basal body in templating cilia formation than currently thought. This raises an important question on the significance and conservation of this process. Until now, the study of this process using stills of TEM sections has prevented the discovery and characterization of faster intermediate steps. *Drosophila* spermatogenesis proved to be a valuable system to study these fast intermediate

stages since central pair assembly takes a few days to be completed. We propose that the presence of singlet MT is a transitory/intermediate state until the second MT of the pair is nucleated. In mature sperm both MTs have equal length (data not shown) and therefore is not obvious that one MT was assembled first. In model organisms often used to study flagella assembly, such intermediate stages might have not been observed due to their transitory nature. In *N. suturalis*, an insect which is phylogenetically close to *D. melanogaster*, a singlet MT has also been observed (LaFountain, 1976) (**Figure S8**). The presence of stages where a singlet MT is easily found can be a consequence of a slower central MT pair assembly rate in these insects.

It is intriguing that during *Drosophila* spermatogenesis the central MT pair starts to assemble so early within the basal body/cilium complex. We conducted an extensive literature search for ultrastructural studies on sperm flagella assembly in other species in order to address whether this was a conserved phenomenon (findings summarized in **Figure S8**). Surprisingly, in both vertebrate and invertebrate species, central MT pairs have been observed in cilia/flagella that assemble during spermatocyte stages, before meiosis I or II respectively (**Figure S8**). Why the central MT pair assembles at that stage, and in particular whether spermatocyte cilia motility is needed for spermatogenesis, is an important question that deserves further study. It is still unclear whether in these different species the central MT pairs found in spermatocyte cilia/flagella are precursors of the central MT pair of sperm flagella, as we describe here for *Drosophila*.

The central MT pair of axonemes is a complex machinery that articulates with the axonemal MT doublets to coordinate flagella movement (Smith and Yang, 2004). Although much is known about the different components of this machinery, little is understood about the molecular regulation of central MT pair nucleation. In light of our findings, we propose BLD10/CEP135 to be one of the first components regulating the initiation of central MT pair biogenesis through MT stabilization. We propose Bld10 conserved N-terminal domain to play

an important role in this process; however, given that removal of that domain does not completely abolish Bld10 activity (Figure 6), we cannot exclude that other Bld10 protein regions also stabilize the central MT pair. It is common for MAPs to have different MT binding domains (Culver-Hanlon et al., 2006; Widlund et al., 2011). Since the middle and C-terminus of Bld10 localize independently to centrioles, it is possible they also stabilize MTs associated with the centriole and the central MT pair, an hypothesis that should be investigated in the future. Some other molecules have been suggested to participate in assembly/maintenance of the central MT pair, such as gamma-tubulin, hydin and kinesin-II (Dawe et al., 2007; McKean et al., 2003; Morris and Scholey, 1997). However, it is unclear how and when these molecules are required for this process. It will be important to understand if and how they interplay with Bld10 in this process.

How general is BLD10/CEP135 function? It is possible that BLD10/CEP135 ancestral function is stabilizing special sets of MTs including the centriole triplets and the singlet MT during axoneme central MT pair assembly. BLD10/CEP135 is present in the genome of most organisms that assemble centrioles and flagella but absent from those that lack these organelles, such as higher plants (Carvalho-Santos et al., 2010; Hodges et al., 2010). While a role for BLD10/CEP135 in central MT pair assembly has not been investigated in vertebrates, TSGA10, a BLD10/CEP135 paralogue only present in vertebrates, localizes to the sperm flagella and has been linked to male sterility, further corroborating a role for this family of proteins in flagella assembly (Modarressi et al., 2004; Modarressi et al., 2001). BLD10/CEP135 loss-of-function in several species generates phenotypes associated with centriolar MT defects, including MT triplet loss (Hiraki et al., 2007; Jerka-Dziadosz et al., 2010; Matsuura et al., 2004), and shorter centrioles (Carvalho-Santos et al., 2010; Mottier-Pavie and Megraw, 2009). The link between Bld10 and these specific MT sets is also supported by its localization to the cartwheel spokes and close to the basal body/centriolar MT triplets (in *Chlamydomonas*, human cells and *Drosophila*) (Hiraki et al., 2007; Kleylein-Sohn et al., 2007; Matsuura et al.,

2004; Mottier-Pavie and Megraw, 2009). It is possible that Bld10 also stabilizes the MTs it associates with, at the centriole cartwheel and walls. The lack of basal bodies in *Chlamydomonas* BLD10 mutants might reflect defects both in cartwheel assembly and in the recruitment and/or stabilization of the basal body MTs associated with the cartwheel (Matsuura et al., 2004). This is not the case in *Drosophila*, as centrioles, albeit shorter, are still observed in *Bld10* mutants (Carvalho-Santos et al., 2010; Mottier-Pavie and Megraw, 2009). It is possible that, in the fruit fly, other molecules are redundant with Bld10 in its role of stabilizing cartwheel-associated MTs. In the future, it will be important to understand how Bld10 might stabilize MTs and how its function is regulated in different centriole compartments (cartwheel, lumen, walls) and at different time points, such as during centriole or central MT pair assembly.

Centrioles and axonemes are very special organelles, being much more stable than any other MT-based structures and resistant to MT depolymerizing drugs (Bettencourt-Dias and Glover, 2007). They not only withstand complex MT remodeling environments but in the case of centrioles they also perdure for several cell generations. Additionally, the assembly and stabilization of centrioles and axonemes involves particular MT regulators and post-translational modifications (Bettencourt-Dias and Glover, 2007). We showed that BLD10/CEP135 is a special MT regulator specifically involved in the formation of highly stable and specialized MTs. The discovery of these specialized MAPs, where SAS4/CPAP could also be included, opens the door to an exciting new biology of MT regulation, which we anticipate to be different from that described for cytoplasmic MTs. Moreover, given the importance of centrioles and cilia in development and homeostasis, this work will allow further contextualization of these cellular structures in human disease.

Experimental Procedures

Constructs

Most vectors used in this study were constructed using the Gateway system (Invitrogen). Bld10 fragments (residues 1-163, 164-490 and 491-1059) were cloned into pDONR221 Zeo vector using Bld10 cDNA (LD35990) as template (Carvalho-Santos et al., 2011) and the following primers: 1-163 fragment (N-Bld10), Forward 5' GGGGACAAGTTTGTACAAAAAAGCAGGCTTCATGAATATCAACGATGGTGACTTT 3', Reverse 5' GGGGACCACTTTGTACAAGAAAGCTGGGTCTTAGCCCGAACGCACTGTGGTTATAAA 3', 164-490 fragment (M-Bld10), Forward 5' GGGGACAAGTTTGTACAAAAAAGCAGGCTTCATGATTGCGATGCCAACTACACTG 3', Reverse 5´ GGGGACCACTTTGTACAAGAAAGCTGGGTCTTAGGGGGGCGGCAGTGTCTCATACTG 3', 491-1059 fragment (C-Bld10), Forward 5' GGGGACAAGTTTGTACAAAAAAGCAGGCTTCATGACAGCTTCATCCATTACCTCC 3' and Reverse 5' GGGGACCACTTTGTACAAGAAAGCTGGGTCTTAAAGAGTCTTCGATGGCACCCGGGG 3', 164-1059 fragment (ΔN-Bld10), Forward 5' GGGGACAAGTTTGTACAAAAAAGCAGGCTTCATGATTGCGATGCCAACTACACTG 3' and Reverse 5' GGGGACCACTTTGTACAAGAAAGCTGGGTCTTAAAGAGTCTTCGATGGCACCCGGGG 3'. The sequence integrity was confirmed by automated sequencing prior to recombination into pMT N-terminal GFP (provided by João Rocha, U. Cambridge). The resulting vectors were used to express the corresponding proteins in *Drosophila* cells Bld10 residues 1-163 were cloned into the pTriEx2/Ampicillin vector (Oxford Protein Production Facility UK) for expression in *E. coli* Rosetta cells using standard cloning techniques. Bld10 residues 164-1059 were cloned into poliUb N-terminal GFP for expression in flies (kindly provided by Renata Basto, Institut Curie, France). Full length GFP-Bld10 constructs for expression in cells and flies were previously described (Carvalho-Santos et al., 2010).

Protein production in and purification from *E. coli*

Cells were grown in Power Broth for 1 h at 37°C and 130 rpm, followed by a temperature shift to 30°C to 1.5 OD (600 nm). Cells were grown at 18°C to OD 2.0, after which cultures where

induced with 0.5 mM IPTG for 18 - 20 hours. Cells were then harvested by centrifugation at 10000 g for 10 min at 4°C. Harvested cells were resuspended in lysis buffer (50 mM KPi pH 6.0, 300 mM NaCl, 10 mM Imidazole, supplemented with Benzonase (10 U/mL), and EDTA-free protease inhibitors), and broken twice in a French Pressure Cell at 131 MPa. After centrifugation for 45 min at 4°C and 27200 g, the supernatant was filtered through a 0.2 μm filter. The soluble fraction was subsequently loaded at 3 ml/min onto a 5 ml Ni-NTA column (Quiagen), previously equilibrated with lysis buffer freshly supplemented with 1 mM 2-mercaptoethanol. Proteins were eluted in a stepwise manner with increasing concentrations of imidazole, followed by ultrafiltration-mediated concentration (Amicon , 10 kDa cutoff), and loaded onto a pre-equilibrated (50 mM Kpi pH 7.5, 300 mM NaCl, 5 mM EDTA, 1 mM 2-mercaptoethanol) Superdex 75 column (XK 16/60; GE Healthcare). All relevant protein peaks were analyzed by SDS-PAGE with Coomassie staining.

Microtubule pelleting assay

MTs were prepared by incubating 100 μl of 100 μM purified MAP-free bovine brain α/β-tubulin (Cytoskeleton) with 2 μl of 50 mM GTP (Sigma-Aldrich) and 0,4 μl of 1M $MgCl_2$ for 30 min at 37 °C. Taxol (Sigma-Aldrich) was added to a final concentration of 20 μM. Samples were centrifuged at 125600 g for 25 min in an Airfuge (Beckman) and the pellet resuspended in 100 μl BRB80 (80 mM PIPES 6.8; 1 mM EGTA; 1 mM $MgCl_2$) supplemented with 20 μM taxol and incubated O/N at RT. The MT μM concentration used in the pelleting assays was calculated as follows: [tubulin] = A280/ε, where the absorption coefficient (ε) for tubulin = 0.10583. For the pelleting assays, 50 μl samples (in BRB80) containing 1,5 μM MTs , 20 μM Taxol, and Ethe-1 or N-Bld10 (final concentrations equaling 0; 0,05; 0,1; 0,25; 0,5 and 1 μM) were incubated for 20 min at 37 °C. Samples were then centrifuged at 108700 g for 20 min in an Airfuge (Beckman). After centrifugation, supernatants and pellets were analyzed by standard Western blot procedures. The signal was detected with mouse anti-α tubulin B512

(Sigma) and mouse anti-His antibodies (Novagen), followed by IRDye 800CW anti-mouse. The Odyssey Scanner system was used for signal quantification.

Microtubule overlay assay

Recombinant proteins (500 ng/lane) were fractionated on 12% SDS-PAGE gels and blotted onto PVDF membranes. The membranes were pre-incubated overnight in TBST (50 mM Tris, pH 7.5, 150 mM NaCl, 0.05% Tween 20) supplemented with 5% low fat powdered milk, and then washed three times for 15 min in lysis buffer (0.1 M PIPES/NaOH, pH 6.6, 5 mM EGTA, 1 mM MgSO4, 0.9 M glycerol, 1 mM DTT and protease inhibitors). The blots were then incubated for 30 min in lysis buffer containing 2 mM GTP. MAP-free bovine brain tubulin (Cytoskeleton) was polymerized at a concentration of 200 nM in lysis buffer supplemented with 1 mM GTP, and incubated at 37°C for 40 min. The membranes were then sequentially incubated for 1 h at 37°C in a buffer containing these polymerized MTs, and for 30 min in 10 µM taxol BRB80. The blots were washed three times with TBST, and the bound tubulin was detected with anti–β-tubulin antibodies (Sigma), and ECL system (GE Healthcare) using standard Western blot procedures.

Fly Stocks and husbandry

The PBac{PB}CG17081^{c04199} *Bld10* mutant allele (Thibault et al., 2004) was used in this study. The original stock had a lethal second mutation which was cleaned. The phenotype of the homozygous flies regarding fertility and central pair defects are indistinguishable from those of the hemizygous mutants (Carvalho-Santos et al., 2011). All analyses were performed using homozygous flies and we refer to those as *Bld10* throughout the text. Transgenic flies expressing GFP-Bld10 have been previously described (Carvalho-Santos et al., 2011), and flies expressing GFP-ΔN-Bld10 were originated by injection of the plasmid constructs (http://www.thebestgene.com). Expression of the transgenes was confirmed by Western Blot and samples were prepared using ten pairs of testes resuspended directly into Laemmli Buffer. RFP-PACT transgenic flies were kindly provided by Jordan Raff (Gurdon Institute, Cambridge,

UK) (Lucas and Raff, 2007). W1118 stocks were used as wild type. All flies were reared according to standard procedures.

***Drosophila* male fertility tests**

Fertility tests were performed by crossing a single male with three wild type females during three days. The progeny per tube was scored and averaged for 10-20 males. A normalized progeny ratio was calculated using the progeny of the correspondent heterozygous mutant as control to eliminate any fertility issue that may have arisen from the insertion of the transgene into the genome (progeny of *Bld10*/*Bld10* divided by progeny of *Bld10*/TM6B; progeny of GFP-Bld10/CyO,*Bld10*/*Bld10* divided by the progeny of GFP-Bld10/CyO,*Bld10*/TM6B and progeny of GFP-ΔN-Bld10/CyO,*Bld10*/*Bld10* divided by the progeny of GFP-ΔN-Bld10/CyO,*Bld10*/TM6B). This assay is quantitatively different from what we have published before regarding the fertility of GFP-Bld10/CyO,*Bld10*/*Bld10* flies (Carvalho-Santos et al., 2011) where we were only scoring the proportion of males which could generate viable progeny (instead of progeny number).

Colchicine feeding

Fly food was prepared with 1 μM of colchicine. Two days are required for a stem cell to originate a cyst of 16 primary spermatocytes, which will then be delayed in G2 stage for ~3 days. The process of spermatogenesis (from a stem cell to mature sperm) lasts 250 hours (~10,5 days). We reasoned that if flies were fed with colchicine-containing food for a period of 7-9 days, germ cells would be exposed to the drug throughout the process of central MT pair formation. 3-4 males (in the presence of females for constant sperm removal) were kept in food without (control) or with colchicine for 7-9 days. Food tubes were changed every two days during the course of the experiment and flies were kept in the dark at room temperature.

Transfection of constructs and colchicine treatment

Drosophila (Dmel) cells were maintained at 25°C in Express 5 SFM (Gibco) supplemented with 1 X L-Glutamine-Penicillin-Streptomycin (Gibco), according to standard tissue-culture

techniques. To transiently transfect cells we used the following protocol: 3 x10^6 cells were plated per well (6-well plate) in 3ml medium; 1 h later cells were transfected. We used either 3 µg plasmid DNA construct of interest mixed with 15 µl Fugene (Promega) and Express 5 SFM up to 100 µl, or 400 ng of plasmid DNA construct of interest mixed with 100 µl EC buffer, 3,2 µl Enhancer, 10 µl Effectene (Roche), and 600 µl of Express 5 SFM. These mixtures were incubated at RT for 15 min, and then added to cells. Cells were allowed to express the constructs for 3 days, in the absence or presence of 500 µM $CuSO_4$. Colchicine treatments were performed just prior to the immunostaining protocol. Briefly, after seeding the cells, 15 µM colchicine (Sigma) were added to each well for 90 min. Fixation was also carried out in the presence of 15 µM colchicine.

Immunostaining and Imaging

Drosophila cells were plated onto glass coverslips, allowed to attach for 1 h, and fixed in 4% formaldehyde in PHEM buffer (60 mM PIPES, 25 mM HEPES, 10 mM EGTA, 4 mM $MgCl_2$). Cells were permeabilized and washed in PBS containing 0,01% Triton and 1% BSA, and stained for Pericentrin-like protein (D-PLP) or acetylated tubulin. DNA was counterstained and coverslips were mounted in DAPI Vectashield mounting medium (H-1200, Vector Laboratories). Samples imaging and phenotype scoring were performed on DeltaVision microscope equipped with EMCCD camera. Images were acquired as a Z-series (0.3 µm apart) and are presented as maximum-intensity projections.

Testes from adults were dissected in 183 mM KCl, 47 mM NaCl, 1 mM EDTA and 10 mM Tris-HCl (pH 6.8), transferred to poly-L-lysine glass slides (Sigma) and frozen in liquid nitrogen as previously described (Cenci et al., 1994). Fixation was done for 8 minutes in dry ice-cold methanol followed by 10 minutes in acetone. DNA was stained with DAPI. Testes were mounted using Vectashield mounting media (Vector Laboratories). Samples were imaged as a Z-series (0.3 µm apart) on a confocal scanning unit motorized CSU-X1 (Yokogawa) coupled to an inverted microscope Nikon Eclipse Ti-E (Nikon) equipped with a Evolve EMCCD camera

(Photometrics). Images are presented as maximum-intensity projections. All figure panels were prepared for publication using Adobe Photoshop (Adobe Systems).

Transmission Electron Microscopy Analysis of Testes and Cells

Testes were dissected from 25-36 h post-puparium stage males for the description of singlet MT assembly, from 0-1 day old adult males for the rescue experiment, and from 7-9 day old flies for the colchicine-feeding experiment. Testes were fixed in 2,5% glutaraldehyde in PBS (pH 7,2) for 2 hrs at 4°C. All samples were post-fixed in 1% OsO_4 for 1 h, and treated with 1% uranyl acetate for 30 min. Samples were then sequentially dehydrated in a graded series of alcohols (70%, 90%, and three times in 100%, for 10 min each). Testes were incubated in propylene oxide three times for 10 min, followed by a double incubation (15 min each) in 1:1 propylene-oxide:resin. Samples were infiltrated for 1 h in pure resin and polymerized for 16-48 h at 60°C. Serial thin sections (60-80nm) were cut in a Leica Reichert Ultracut S ultramicrotome, collected on formvar-coated copper slot grids, and stained with uranyl acetate and lead citrate (Hayat, 1989). Samples were examined and photographed at 80kV using either a JEOL CX-100 II or a Hitachi 7650 electron microscope. All the experiments where we show flagellar axonemes were imaged and analyzed from early spermatids. This specific stage was identified by the presence of the centriolar adjunct (thin aggregate around the full length of the basal body) and the two immature mitochondrial derivatives (as shown in **Figure 2, 3** and **Movies S3-4**). At these stages, the axoneme has just begun elongation, thus being the critical stage where to look for the early steps of central pair formation.

Cultured cells were plated onto Aclar membranes and fixed in 2,5% glutaraldehyde in PBS (pH 7,2) supplemented with 0,2% Triton X-100 for 2h at RT to facilitate visualization of the MTs. The next steps were the same as reported above for testes samples.

Electron tomography and image analysis

Serial sections (130-150 nm) were collected onto formvar-coated copper slot grids. Single axis tilt series of basal bodies were collected at +-60° with 1° increments, at 120 kV using a Hitachi

7650 electron microscope. The IMOD package 4.1.6 was used for tomogram generation and 3D modeling (Mastronarde, 1997).

Antibodies

An antibody was raised in rabbit against the 330-580 residues of Bld10 (Metabion). The antibodies and dilutions used in this study were the following: Chicken anti-*Drosophila* PLP (1:1000, (Rodrigues-Martins et al., 2007b)), mouse anti-acetylated tubulin (1:1000, Sigma), mouse anti-α tubulin B512 (1:200000, Sigma), mouse anti–β-tubulin (1:7000, Sigma), mouse anti-GFP (1:200, Roche), rabbit anti-GFP (1:1000, Abcam), mouse anti-His (1:1000, Novagen), and rabbit anti-Bld10 (1:750). Secondary antibodies were purchased from Jackson Immunoresearch Laboratories and LI-COR, and used at 1:100 for immunostaining or 1:10000 for Western Blot.

Bibliography

Bettencourt-Dias, M., and Glover, D.M. (2007). Centrosome biogenesis and function: centrosomics brings new understanding. Nature reviews *8*, 451-463.

Bettencourt-Dias, M., Hildebrandt, F., Pellman, D., Woods, G., and Godinho, S.A. (2011). Centrosomes and cilia in human disease. Trends Genet *27*, 307-315.

Blachon, S., Cai, X., Roberts, K.A., Yang, K., Polyanovsky, A., Church, A., and Avidor-Reiss, T. (2009). A proximal centriole-like structure is present in Drosophila spermatids and can serve as a model to study centriole duplication. Genetics *182*, 133-144.

Braun, M., Drummond, D.R., Cross, R.A., and McAinsh, A.D. (2009). The kinesin-14 Klp2 organizes microtubules into parallel bundles by an ATP-dependent sorting mechanism. Nature cell biology *11*, 724-730.

Carvalho-Santos, Z., Azimzadeh, J., Pereira-Leal, J.B., and Bettencourt-Dias, M. (2011). Evolution: Tracing the origins of centrioles, cilia, and flagella. The Journal of cell biology *194*, 165-175.

Carvalho-Santos, Z., Machado, P., Branco, P., Tavares-Cadete, F., Rodrigues-Martins, A., Pereira-Leal, J.B., and Bettencourt-Dias, M. (2010). Stepwise evolution of the centriole-assembly pathway. Journal of cell science *123*, 1414-1426.

Cenci, G., Bonaccorsi, S., Pisano, C., Verni, F., and Gatti, M. (1994). Chromatin and microtubule organization during premeiotic, meiotic and early postmeiotic stages of Drosophila melanogaster spermatogenesis. Journal of cell science *107 (Pt 12)*, 3521-3534.

Culver-Hanlon, T.L., Lex, S.A., Stephens, A.D., Quintyne, N.J., and King, S.J. (2006). A microtubule-binding domain in dynactin increases dynein processivity by skating along microtubules. Nature cell biology *8*, 264-270.

Dawe, H.R., Shaw, M.K., Farr, H., and Gull, K. (2007). The hydrocephalus inducing gene product, Hydin, positions axonemal central pair microtubules. BMC biology *5*, 33.

Dobbelaere, J., Josue, F., Suijkerbuijk, S., Baum, B., Tapon, N., and Raff, J. (2008). A genome-wide RNAi screen to dissect centriole duplication and centrosome maturation in Drosophila. PLoS biology *6*, e224.
Dute, R., and Kung, C. (1978). Ultrastructure of the proximal region of somatic cilia in Paramecium tetraurelia. The Journal of cell biology *78*, 451-464.
Fliegauf, M., Benzing, T., and Omran, H. (2007). When cilia go bad: cilia defects and ciliopathies. Nature reviews *8*, 880-893.
Fritz-Niggli, H., and Suda, T. (1972). Bildung und Bedeutung der Zentriolen: Eine Studie und Neuinterpretation der Meiose von Drosophila. Cytobiologie *5*, 12-41.
Fuller, M.T. (1998). Genetic control of cell proliferation and differentiation in Drosophila spermatogenesis. Semin Cell Dev Biol *9*, 433-444.
Geimer, S., and Melkonian, M. (2004). The ultrastructure of the Chlamydomonas reinhardtii basal apparatus: identification of an early marker of radial asymmetry inherent in the basal body. Journal of cell science *117*, 2663-2674.
Hayat, M. (1989). Principles and techniques of Electron Microscopy: Biological Applications (Basingtoke, Macmillan Press Ltd.).
Hibberd, D.J. (1975). Observations on the ultrastructure of the choanoflagellate Codosiga botrytis (Ehr.) Saville-Kent with special reference to the flagellar apparatus. Journal of cell science *17*, 191-219.
Hiraki, M., Nakazawa, Y., Kamiya, R., and Hirono, M. (2007). Bld10p constitutes the cartwheel-spoke tip and stabilizes the 9-fold symmetry of the centriole. Curr Biol *17*, 1778-1783.
Hodges, M.E., Scheumann, N., Wickstead, B., Langdale, J.A., and Gull, K. (2010). Reconstructing the evolutionary history of the centriole from protein components. Journal of cell science *123*, 1407-1413.
Hsu, W.B., Hung, L.Y., Tang, C.J., Su, C.L., Chang, Y., and Tang, T.K. (2008). Functional characterization of the microtubule-binding and -destabilizing domains of CPAP and d-SAS-4. Experimental cell research *314*, 2591-2602.
Hung, L.Y., Chen, H.L., Chang, C.W., Li, B.R., and Tang, T.K. (2004). Identification of a novel microtubule-destabilizing motif in CPAP that binds to tubulin heterodimers and inhibits microtubule assembly. Molecular biology of the cell *15*, 2697-2706.
Inoue, Y.H., do Carmo Avides, M., Shiraki, M., Deak, P., Yamaguchi, M., Nishimoto, Y., Matsukage, A., and Glover, D.M. (2000). Orbit, a novel microtubule-associated protein essential for mitosis in Drosophila melanogaster. The Journal of cell biology *149*, 153-166.
Jerka-Dziadosz, M., Gogendeau, D., Klotz, C., Cohen, J., Beisson, J., and Koll, F. (2010). Basal body duplication in Paramecium: the key role of Bld10 in assembly and stability of the cartwheel. Cytoskeleton (Hoboken) *67*, 161-171.
Kleylein-Sohn, J., Westendorf, J., Le Clech, M., Habedanck, R., Stierhof, Y.D., and Nigg, E.A. (2007). Plk4-induced centriole biogenesis in human cells. Developmental cell *13*, 190-202.
Kohlmaier, G., Loncarek, J., Meng, X., McEwen, B.F., Mogensen, M.M., Spektor, A., Dynlacht, B.D., Khodjakov, A., and Gonczy, P. (2009). Overly long centrioles and defective cell division upon excess of the SAS-4-related protein CPAP. Curr Biol *19*, 1012-1018.
LaFountain, J.R., Jr. (1976). Analysis of birefringence and ultrastructure of spindles in primary spermatocytes of Nephrotoma suturalis during anaphase. J Ultrastruct Res *54*, 333-346.
Lucas, E.P., and Raff, J.W. (2007). Maintaining the proper connection between the centrioles and the pericentriolar matrix requires Drosophila centrosomin. The Journal of cell biology *178*, 725-732.
Martinez-Campos, M., Basto, R., Baker, J., Kernan, M., and Raff, J.W. (2004). The Drosophila pericentrin-like protein is essential for cilia/flagella function, but appears to be dispensable for mitosis. The Journal of cell biology *165*, 673-683.
Mastronarde, D.N. (1997). Dual-axis tomography: an approach with alignment methods that preserve resolution. Journal of structural biology *120*, 343-352.

Matsuura, K., Lefebvre, P.A., Kamiya, R., and Hirono, M. (2004). Bld10p, a novel protein essential for basal body assembly in Chlamydomonas: localization to the cartwheel, the first ninefold symmetrical structure appearing during assembly. The Journal of cell biology *165*, 663-671.
McKean, P.G., Baines, A., Vaughan, S., and Gull, K. (2003). Gamma-tubulin functions in the nucleation of a discrete subset of microtubules in the eukaryotic flagellum. Curr Biol *13*, 598-602.
Modarressi, M.H., Behnam, B., Cheng, M., Taylor, K.E., Wolfe, J., and van der Hoorn, F.A. (2004). Tsga10 encodes a 65-kilodalton protein that is processed to the 27-kilodalton fibrous sheath protein. Biology of reproduction *70*, 608-615.
Modarressi, M.H., Cameron, J., Taylor, K.E., and Wolfe, J. (2001). Identification and characterisation of a novel gene, TSGA10, expressed in testis. Gene *262*, 249-255.
Morris, R.L., and Scholey, J.M. (1997). Heterotrimeric kinesin-II is required for the assembly of motile 9+2 ciliary axonemes on sea urchin embryos. The Journal of cell biology *138*, 1009-1022.
Mottier-Pavie, V., and Megraw, T.L. (2009). Drosophila bld10 is a centriolar protein that regulates centriole, basal body, and motile cilium assembly. Molecular biology of the cell *20*, 2605-2614.
Nigg, E.A., and Raff, J.W. (2009). Centrioles, centrosomes, and cilia in health and disease. Cell *139*, 663-678.
Rodrigues-Martins, A., Bettencourt-Dias, M., Riparbelli, M., Ferreira, C., Ferreira, I., Callaini, G., and Glover, D.M. (2007a). DSAS-6 Organizes a Tube-like Centriole Precursor, and Its Absence Suggests Modularity in Centriole Assembly. Curr Biol.
Rodrigues-Martins, A., Riparbelli, M., Callaini, G., Glover, D.M., and Bettencourt-Dias, M. (2007b). Revisiting the role of the mother centriole in centriole biogenesis. Science (New York, NY *316*, 1046-1050.
Schmidt, T.I., Kleylein-Sohn, J., Westendorf, J., Le Clech, M., Lavoie, S.B., Stierhof, Y.D., and Nigg, E.A. (2009). Control of centriole length by CPAP and CP110. Curr Biol *19*, 1005-1011.
Silflow, C.D., Liu, B., LaVoie, M., Richardson, E.A., and Palevitz, B.A. (1999). Gamma-tubulin in Chlamydomonas: characterization of the gene and localization of the gene product in cells. Cell motility and the cytoskeleton *42*, 285-297.
Smith, E.F., and Yang, P. (2004). The radial spokes and central apparatus: mechano-chemical transducers that regulate flagellar motility. Cell motility and the cytoskeleton *57*, 8-17.
Tang, C.J., Fu, R.H., Wu, K.S., Hsu, W.B., and Tang, T.K. (2009). CPAP is a cell-cycle regulated protein that controls centriole length. Nature cell biology *11*, 825-831.
Tates, A.D. (1971). Cytodifferentiation during spermatogenesis in *Drosophila melanogaster*: an electron microscope study. (Leiden, Netherlands, Rijksuniversiteit de Leiden).
Thibault, S.T., Singer, M.A., Miyazaki, W.Y., Milash, B., Dompe, N.A., Singh, C.M., Buchholz, R., Demsky, M., Fawcett, R., Francis-Lang, H.L*., et al.* (2004). A complementary transposon tool kit for Drosophila melanogaster using P and piggyBac. Nature genetics *36*, 283-287.
Widlund, P.O., Stear, J.H., Pozniakovsky, A., Zanic, M., Reber, S., Brouhard, G.J., Hyman, A.A., and Howard, J. (2011). XMAP215 polymerase activity is built by combining multiple tubulin-binding TOG domains and a basic lattice-binding region. Proceedings of the National Academy of Sciences of the United States of America *108*, 2741-2746.

Acknowledgements

We thank Giuliano Callaini, Tim Megraw, Helio Roque, and Jordan Raff for discussions and sharing unpublished data. We would like to thank Nikola Dzhindzhev, Erika LF. Holzbaur, Bryan

Tsou, Ryoko Kuriyama, Clare Waterman Storer, Fanni Gergely, Fernando Bazan, Catarina Samora and Andrew McAinsh and members of the MBD laboratory for discussions and suggestions. We thank Alex Dammerman, Monica Gotta, Jose Pereira-Leal, Rui Martinho, Patrick Meraldi, Inês Bento and Daniela Brito for critically reading the manuscript. We would like to thank the European Commission Framework Program 7 project P-CUBE (Louise Bird, OPPF-UK) for the protein expression screening, Cláudio Gomes (ITQB/Universidade Nova de Lisboa) for providing us with pure Ethe-1 and Tang K. Tang (Institute of Biomedical Sciences, Academia Sinica, Taipei 11529, Taiwan) for providing pure CPAP microtubule-binding domain. We thank Bloomington Stock Center and BestGene Inc. for fly stocks. We thank Sabine Pruggnaller (EMBL) for helping on tomogram generation and 3D modeling and David Mastronarde (The Boulder Laboratory for 3D Electron Microscopy of Cells, University of Colorado) for technical support for the IMOD software package. This work was funded by Fundação para a Ciência e Tecnologia (FCT): PTDC/BIA-BCM/105602/2008 and an EMBO Installation Grant (co-funded by FCT and Instituto Gulbenkian de Ciência). Authors are funded by Ciência 2007 program, ERC, FCT, EMBO and Marie Curie Actions fellowships.

Figure Legends

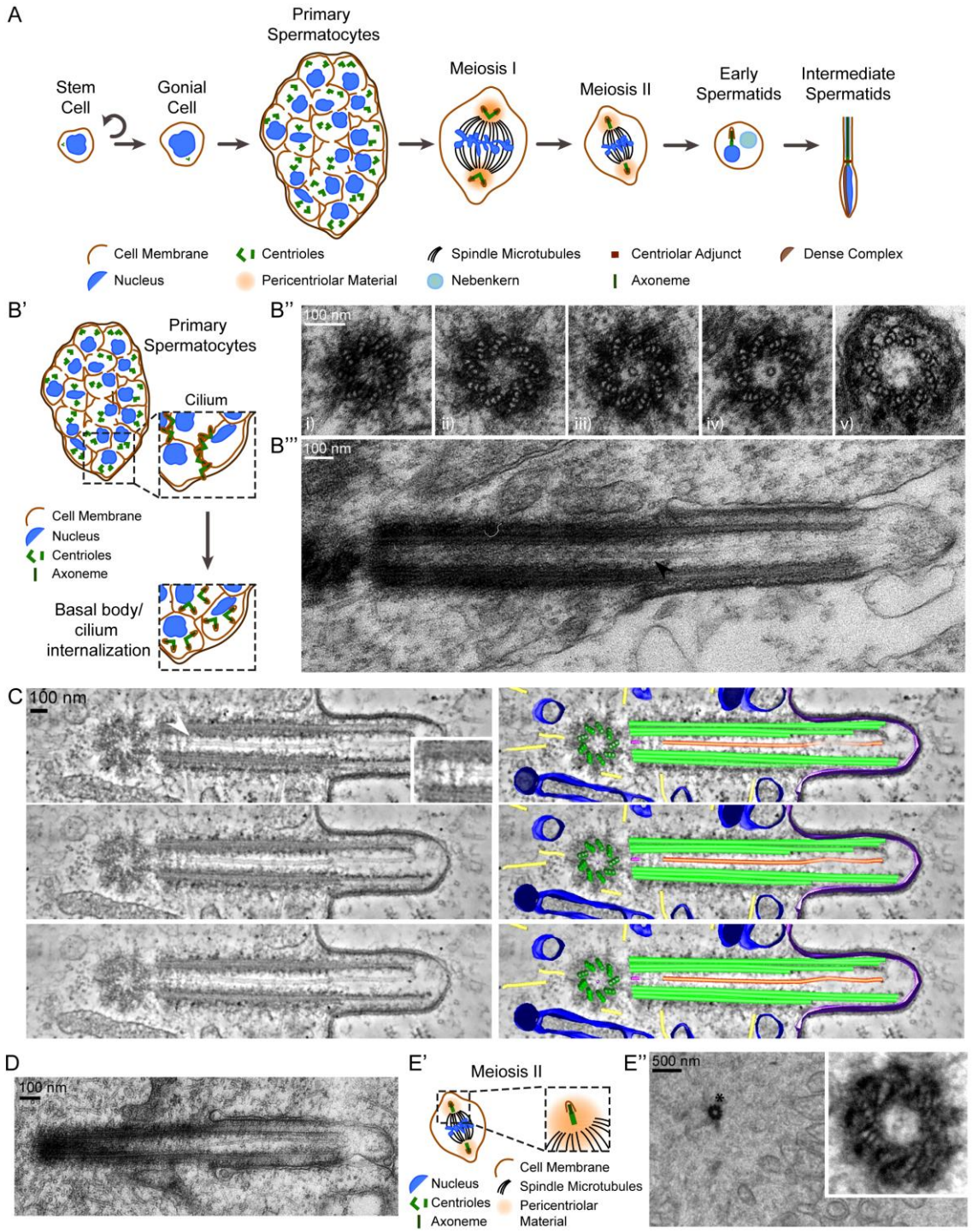

Figure 1 – The central MT pair of the motile axoneme starts to assemble within the small cilium of primary spermatocytes. A. Schematic representation of *Drosophila* spermatogenesis. The division of a stem cell originates a gonial cell that undergoes four rounds of incomplete mitotic divisions to produce a 16-cell cyst of primary spermatocytes. Primary spermatocytes undergo a long G2 phase, during which centrioles elongate and migrate to the cell membrane where they grow a cilium (Fritz-Niggli and Suda, 1972; Tates, 1971). Each spermatocyte then undergoes two consecutive meiotic divisions without DNA

replication and centriole duplication. Early spermatids are the result of these meiotic divisions, each containing a single basal body nucleating the sperm flagellum. **B', B''** and **B'''.** A MT singlet is present within the basal body/cilium of primary spermatocytes. **B'.** Schematic representation of G2 spermatocytes where the small cilium assembles and is internalized before meiosis. **B''.** Representative TEM cross sections of a G2 spermatocyte basal body and cilium, from the most proximal (left) to the most distal (right) region. Note that, in this case, the singlet MT is only seen within the basal body. **i)** centriole cartwheel**; ii)** singlet MT is not present; **iii)** and **iv)** sections through the basal body showing the singlet MT; **v)** ciliary axoneme (doublet structure) without singlet MT. See **Figure S1** for the complete series. **B'''.** Longitudinal section of a primary spermatocyte cilium containing a singlet MT (indicated by a black arrowhead). Note that this MT runs continuously within basal body and axoneme. **C.** Left panel: longitudinal tomogram stills of a small cilium from a G2 spermatocyte. The white arrowhead indicates the beginning of the singlet MT. Inset corresponds to 1,5X magnification of the region marked by an arrowhead. Right panel: schematic model based on and overlaying the tomogram data. The singlet MT is represented in red, the basal body and flagellar MT walls are shown in green, the microtubules nucleated from the basal bodies are in yellow, the cartwheel hub is in purple, the vesicles are represented in blue and the cell/ciliary membranes are in dark purple. Note that the tip of the singlet MT is tapered and is discontinuous from the cartwheel hub. Also, note that the singlet MT is bent, justifying the importance of tomograms in this analysis since these structures might be less obvious in single sections. For the complete tomogram see **Movie S1**. The complexity of the cartwheel structure is better detailed in **Movies S1-2**. **D**. Cilia are internalized before meiosis. Longitudinal section of a G2 cilium after incorporation into the cytoplasm while still surrounded by the ciliary membrane. Note the presence of the singlet MT. **E'-E''.** Secondary spermatocytes undergoing meiosis II have a singlet MT. **E'.** Schematic representation of this stage. **E''.** Representative TEM image. Inset corresponds to an 8X magnification of the region indicated by a black asterisk.

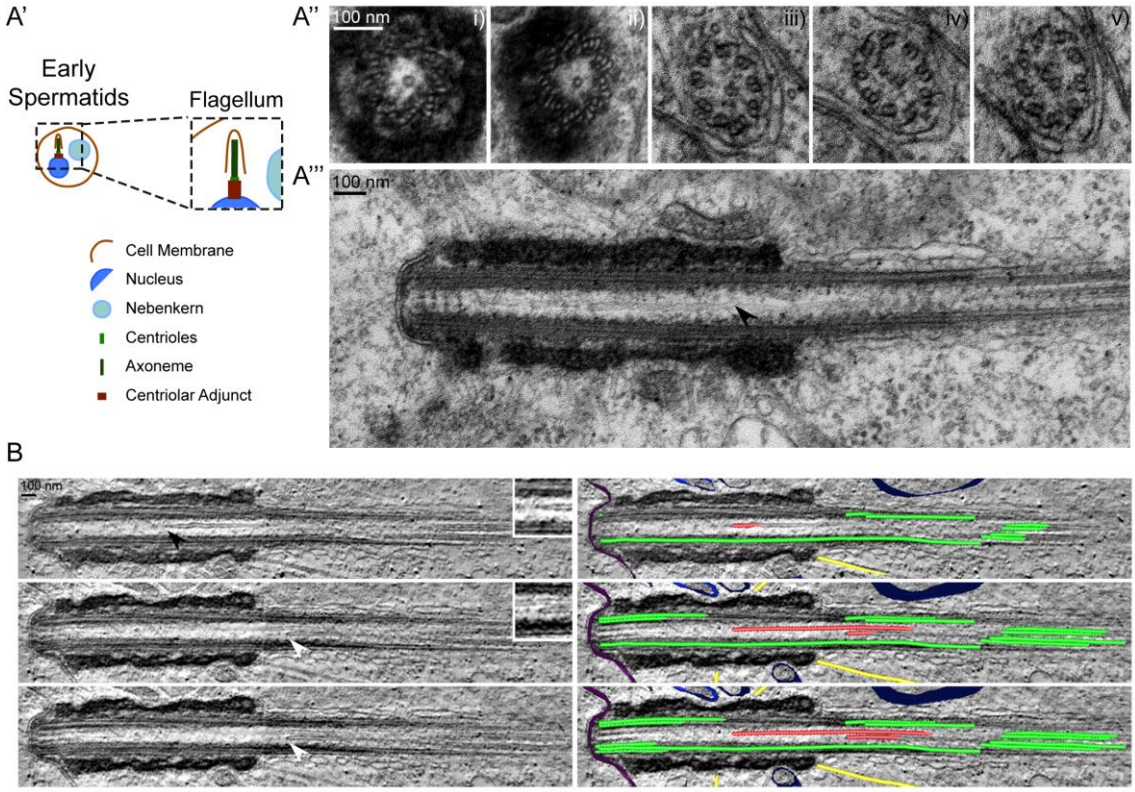

Figure 2 – The singlet MT that forms within the basal body extends into, and is part of, the sperm flagellum central MT pair in early stages of central pair formation. **A', A'', A'''.** Early spermatid bearing a single basal body nucleating a flagellum. **A'.** Schematic representation of the early spermatid stage. **A''.** Representative TEM cross sections of a basal body/flagellum in an early spermatid, from the most proximal (left) to the most distal (right) region. **i), ii)** basal body region with singlet MT; **iii)** flagellar axoneme region (doublet structure) showing the singlet MT; **iv)** intermediate section before formation of second MT within the pair; **v)** central MT pair. Note that the singlet MT from panel **iii)** corresponds to one of the MTs of the central pair in **v)**. For the complete series see **Figure S2**. **A'''.** Longitudinal section of an early spermatid flagellum. The singlet MT is indicated by the black arrowhead. **B.** Left panel: longitudinal tomogram stills of an early spermatid flagellum. Black arrowhead indicates the tip of the singlet MT, and the white arrowhead indicates the tip of the second MT of the flagellum central pair. Insets correspond to 1,5X magnifications of the regions marked with arrowheads, where the tips of the two MTs are tapered. Right panel: schematic model of the structure based on and overlaying the tomogram data. The singlet and central MT pair are represented in red, the basal body and flagellar MT walls are shown in green, the nuclear membrane is in purple, the Nebenkern (mitochondrial derivative) is in blue, and the microtubules nucleated from the centriolar adjunct around the centriole are represented in yellow. Note the continuity between the central MT and the axoneme central MT pair, reinforcing the hypothesis of this singlet to be a MT. For the complete tomogram see **Movie S3**. See also **Figure S2** and **Movie S4** for other examples.

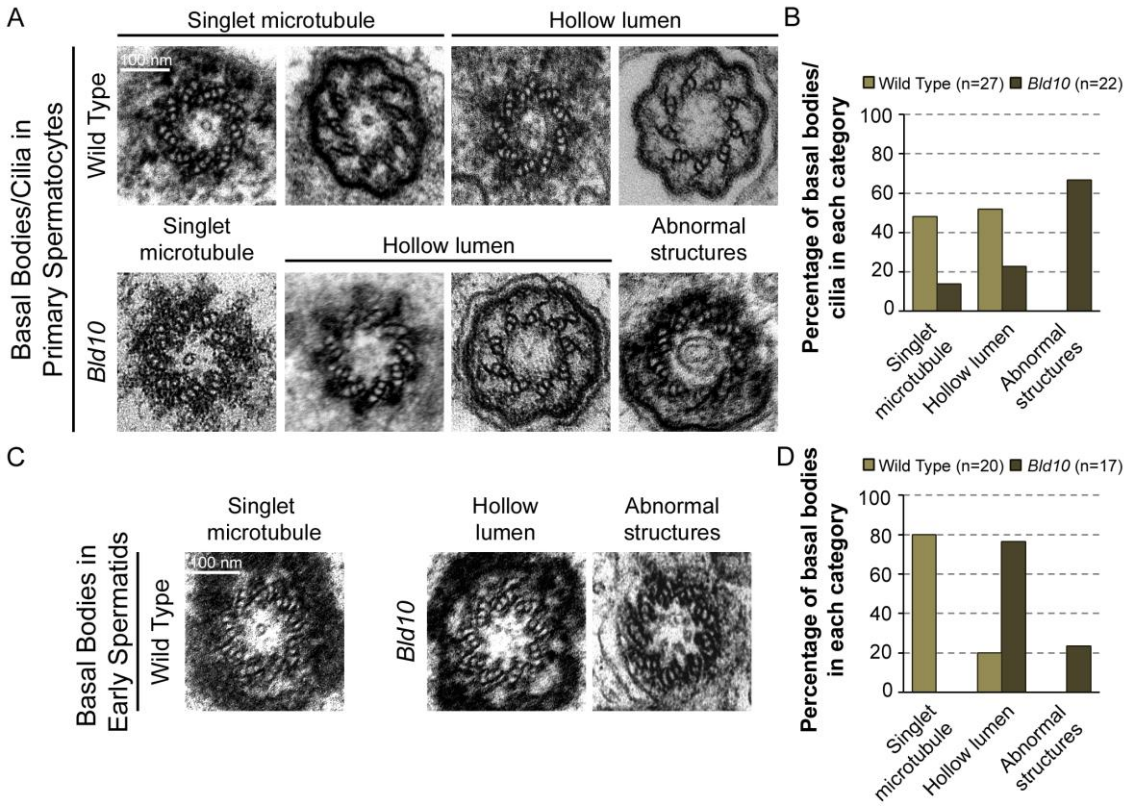

Figure 3 – Bld10 is required for the assembly of the singlet MT. A. Representative TEM cross section images of the structural diversity found in the lumen of WT and *Bld10* basal body/ciliary structures during primary spermatocyte cilium assembly. **B.** Quantification of the different structural phenotypes (as defined in panel **A**). A singlet MT was found within 43% of basal bodies (n=23) and 50% of axonemes (n=22) in the WT. A singlet MT was found within 11% of basal bodies (n=18) and 10% axonemes in *Bld10* mutants (n=10).n represents the number of structures analyzed. *Bld10* data distribution is significantly different from that of the WT (p<0,0001).**C.** Representative cross section TEM images of the structural diversity present in the lumen of WT and *Bld10* basal bodies during early spermatid flagellum assembly (the spermatogenesis staging is described in **Experimental Procedures**). **D.** Quantification of the different structural phenotypes (as defined in panel **C**). n represents the number of structures analyzed. *Bld10* data distribution is significantly different from that of the WT (p<0,0001). Note that the number of structures showing a singlet MT is likely underrepresented, as this analysis was based on discrete longitudinal and cross sections.

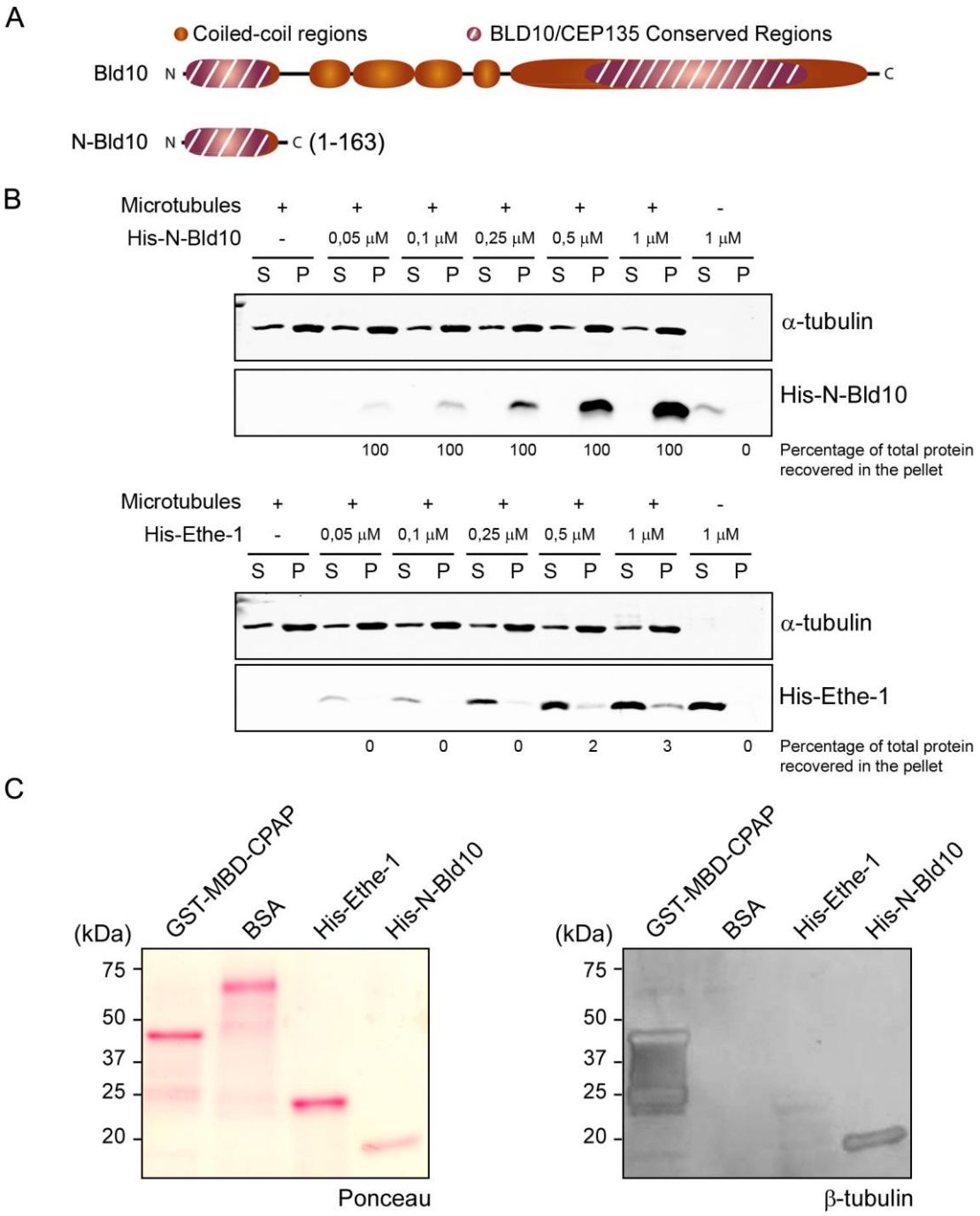

Figure 4 – The Bld10 conserved N-terminal domain binds microtubules *in vitro*. A. Schematic representation of the full length Bld10 and of the N-Bld10 fragment. Note that the latter contains a conserved region and a single predicted coiled-coil (Carvalho-Santos et al., 2010). **B.** Microtubule pelleting assay (see **Experimental Procedures** for details). Assays were performed in the presence (+) or absence (-) of different components. P, pellet fraction containing taxol-stabilized microtubules; S, supernatant fraction containing soluble proteins. His-Ethe-1, a mitochondrial protein, was used as negative control. For all the His-N-Bld10 concentrations tested, we recovered 100% of the protein in the pellet, in a microtubule-dependent manner, contrasting to only a maximum of 3% for His-Ethe-1. Results are representative of two independent experiments. Anti-His antibody was used to detect His-N-Bld10

and His-Ethe-1. **C.** Microtubule overlay assay (see **Experimental Procedures** for details). The MT binding domain (MBD) of CPAP was used as a positive control, while BSA and His-Ethe-1 were used as negative controls. The total amount of the different proteins loaded on the gel is comparable, as shown by Ponceau staining. Note that while GST-MBD-CPAP and His-N-Bld10 bind to microtubules, neither negative control does. The data shown is representative of five independent experiments.

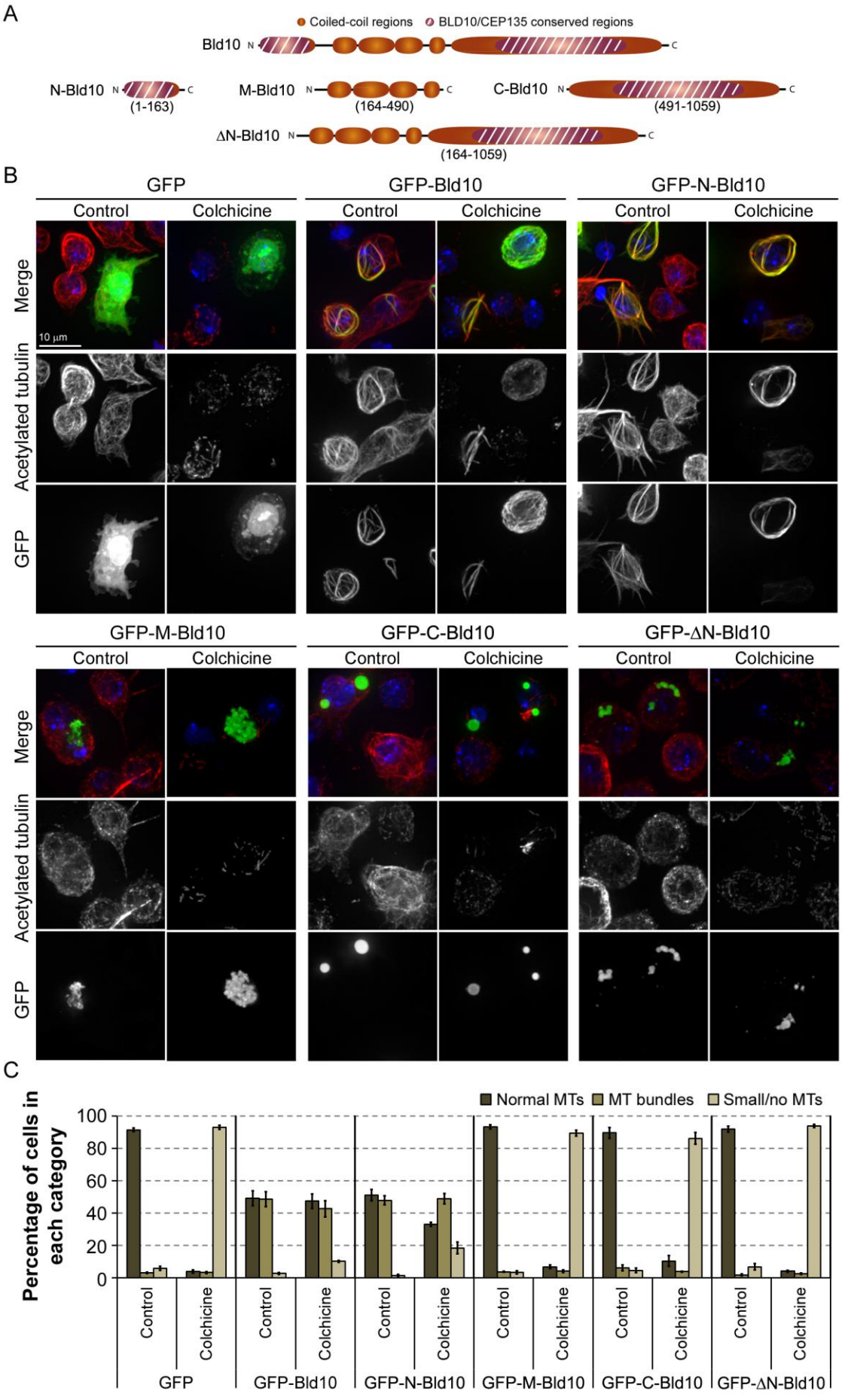
A
Coiled-coil regions
BLD10/CEP135 conserved regions
Bld10
N-Bld10
(1-163)
M-Bld10
(164-490)
C-Bld10
(491-1059)
ΔN-Bld10
(164-1059)
B
GFP
GFP-Bld10
GFP-N-Bld10
GFP-M-Bld10
GFP-C-Bld10
GFP-ΔN-Bld10
Control
Colchicine
Merge
Acetylated tubulin
GFP
10 μm
C
Normal MTs
MT bundles
Small/no MTs
Percentage of cells in each category
100
80
60
40
20
0
Control
Colchicine
GFP
GFP-Bld10
GFP-N-Bld10
GFP-M-Bld10
GFP-C-Bld10
GFP-ΔN-Bld10

Figure 5 – GFP-Bld10 stabilizes cytoplasmic MTs in tissue culture cells through its N-terminal domain. **A.** Schematic representation of full length Bld10, N-, M-, C- and ΔN-Bld10 truncations. The amino acid positions of the two conserved regions and of the region spanning the coiled-coil domains are indicated. Spanning residues for each fragment are indicated in brackets. **B.** *Drosophila* culture cells expressing the different proteins were treated with 15 μM colchicine, a MT depolymerizing agent, for 1,5 hours. Cells were stained for acetylated tubulin (red) and DNA (blue). Note that the expression of either GFP-Bld10 or GFP-N-Bld10 leads to the formation of MT bundles that are colchicine-resistant. See also **Figures S3-4**. Scale bar corresponds to 10 μm. **C.** Quantification of MT phenotypes in cells expressing the different proteins in the presence or absence of colchicine. Results are represented as the mean +/- SEM of three independent experiments. A minimum of 100 cells were scored per condition. Note that the population of cells expressing GFP-Bld10 or GFP-N-Bld10 are significantly different from the control (GFP) regarding their MT cytoskeleton configuration, either in the absence or presence of colchicine ($p<0,0001$).

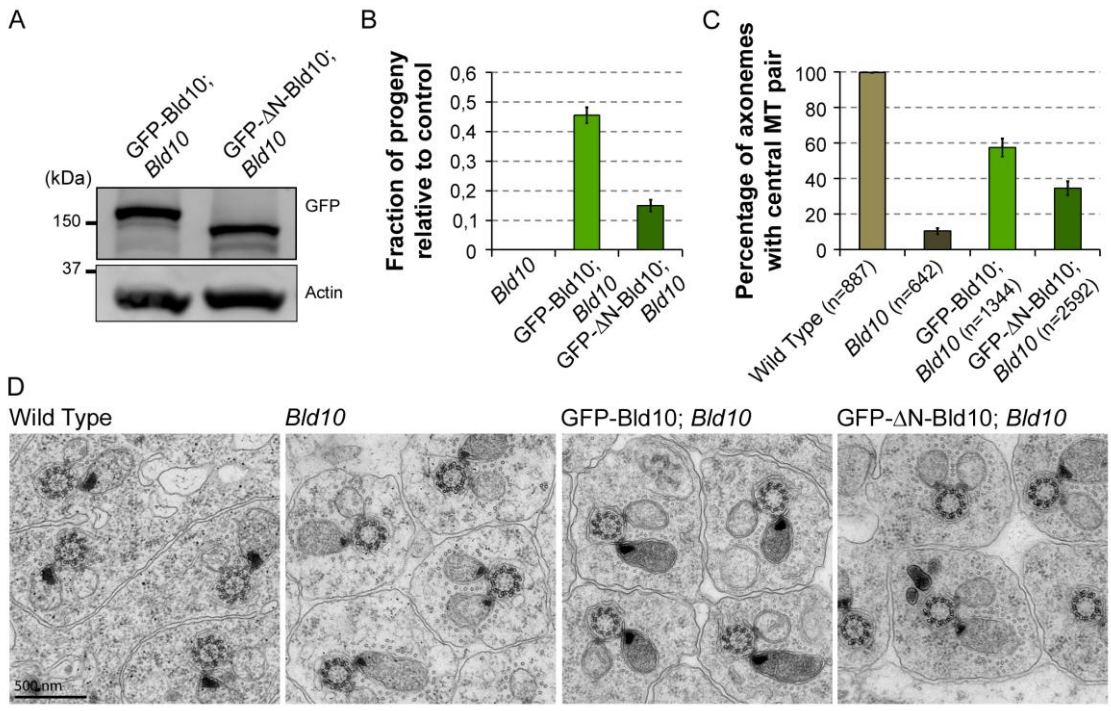

Figure 6 – Microtubule stabilization is important for Bld10 role in central MT pair assembly. **A.** Western Blot showing the expression of either GFP-Bld10 or GFP-ΔN-Bld10 in testes of *Bld10* transgenic lines. The expression of these proteins is driven by the constitutive poliUb promoter. **B.** The N-terminus of Bld10 is important for male fertility. Fertility is represented as the ratio of average progeny per male relative to the control (see **Experimental Procedures** for details). The extent of rescue with the full length GFP-Bld10 is significantly different from that of GFP-ΔN-Bld10 ($p<0,0001$). Similar results were observed with independent transgenic lines. **C.** The N-terminus of Bld10 is important for central pair assembly. The number of axonemes with central MT pair in testes from WT, *Bld10*, GFP-Bld10;*Bld10* (one copy of GFP-Bld10 in Bld10 mutant background) and GFP-ΔN-Bld10;*Bld10* (one copy of GFP-ΔN-Bld10 in Bld10 mutant background) males was scored. n is the total number of axonemes scored. Results correspond to the mean +/- SEM of 3-8 males. The percentage of axonemes with central pair in GFP-ΔN-Bld10;*Bld10* is significantly different from that of GFP-Bld10;*Bld10* ($p<0,0001$). **D.** Representative TEM images of flagellar axonemes in testes of flies with the different genotypes. The fact that we do not obtain full rescue of the mutant with PoliUb GFP-Bld10 might be a consequence of absence of its transcriptional regulation and/or steric hindrance imposed by the GFP tag.